Hybrid stars with the color dielectric and the MIT bag models

C. Maieron, M. Baldo, G. F. Burgio, and H.-J. Schulze
INFN, Sezione di Catania, Via Santa Sofia 64, 95123 Catania, Italy
(Received 29 April 2004; published 27 August 2004)

We study the hadron-quark phase transition in the interior of neutron stars (NS). For the hadronic sector, we use a microscopic equation of state (EOS) involving nucleons and hyperons derived within the Brueckner-Bethe-Goldstone many-body theory, with realistic two-body and three-body forces. For the description of quark matter, we employ both the MIT bag model with a density dependent bag constant, and the color dielectric model. We calculate the structure of NS interiors with the EOS comprising both phases, and we find that the NS maximum masses are never larger than 1.6 solar masses, no matter the model chosen for describing the pure quark phase.

DOI: 10.1103/PhysRevD.70.043010 PACS number(s): 26.60.+c, 21.65.+f, 24.10.Cn, 97.60.Jd

I. INTRODUCTION

The appearance of quark matter in the interior of massive neutron stars (NS) is one of the main issues in the physics of these compact objects. Many equations of state (EOS) have been used to describe the interior of NS, as compiled and discussed in recent review papers [1]. If only nucleonic degrees of freedom are considered and the choice of the EOS is restricted to the microscopic ones [2–4], it turns out that for the heaviest NS, close to the maximum mass (about two solar masses), the central particle density reaches values larger than $1/\mathrm{fm}^3$. In this density range the nucleon cores (dimension ≈ 0.5 fm) start to touch each other, and it is hard to imagine that only nucleonic degrees of freedom can play a role. On the contrary, it can be expected that even before reaching these density values, the nucleons start to lose their identity, and quark degrees of freedom are excited at a macroscopic level.

Unfortunately it is not straightforward to predict the relevance of quark degrees of freedom in the interior of NS for the different physical observables, like cooling evolution, glitch characteristics, neutrino emissivity, and so on. In fact, the other NS components can mask the effects coming directly from quark matter. In some cases the properties of quark and nucleonic matter are not very different, and a clear observational signal of the presence of the deconfined phase inside a NS is indeed hard to find.

The value of the maximum mass of NS is probably one of the physical quantities that is most sensitive to the presence of quark matter in NS. If the quark matter EOS is quite soft, the quark component is expected to appear in NS and to affect appreciably the maximum mass value, which in this case is expected to be slightly larger than the observational limit (1.44 solar masses of the so-called Taylor pulsar [5]). Of course, other ''exotic'' components, in particular hyperons, could also soften the EOS.

On the contrary, the observation of a large NS mass (about 2 solar masses) would imply that the EOS of NS matter is stiff enough to keep the maximum mass at these large values. Purely nucleonic EOS are able to accommodate such large masses [2–4]. Since the presence of non-nucleonic degrees of freedom, like hyperons and quarks, tends usually to soften considerably the EOS with respect to purely nucleonic matter, thus lowering the mass value, their appearance would in this case be incompatible with observations. The large value of the mass could then be explained only if both hyperonic and quark matter EOS are much stiffer than expected. In particular, the quark EOS should be assumed to be stiff enough to render the deconfined phase energetically disfavored.

In this paper we will discuss this issue in detail. Unfortunately, while the microscopic theory of the nucleonic EOS has reached a high degree of sophistication, the quark matter EOS is poorly known at zero temperature and at the high baryonic density appropriate for NS. One has, therefore, to rely on models of quark matter, which contain a high degree of uncertainty. The best one can do is to compare the predictions of different models and to estimate the uncertainty of the results for the NS matter as well as for the NS structure and mass. In this paper we will use a definite nucleonic EOS, which has been developed on the basis of nuclear matter many-body theory, and two different models for the quark EOS, and compare the results. Confrontation with previous calculations shall also be discussed.

The paper is organized as follows: In Sec. II we review the determination of the baryonic EOS comprising nucleons and hyperons in the Brueckner-Hartree-Fock approach. Section III concerns the quark matter EOS according to the MIT bag model and the color dielectric model (CDM). In Sec. IV we present the results regarding neutron star structure combining the baryonic and quark matter EOS for beta-stable nuclear matter. Section V contains our conclusions.

II. BRUECKNER THEORY

A. EOS of nuclear matter

The Brueckner-Bethe-Goldstone (BBG) theory is based on a linked cluster expansion of the energy per nucleon of nuclear matter (see Ref. [6], chapter 1 and references therein). The basic ingredient in this many-body approach is the Brueckner reaction matrix G, which is the solution of the Bethe-Goldstone equation

$$G[\rho;\omega] = v + \sum_{k_a,k_b} v \frac{|k_a k_b\rangle Q \langle k_a k_b|}{\omega - e(k_a) - e(k_b)} G[\rho;\omega], \quad (1)$$

where v is the bare nucleon-nucleon (NN) interaction, ρ is the nucleon number density, and ω the starting energy. The single-particle energy $e(k)$ (assuming $\hbar=1$ here and throughout the paper),

$$e(k)=e(k;\rho)=\frac{k^2}{2m}+U(k;\rho), \tag{2}$$

and the Pauli operator Q determine the propagation of intermediate baryon pairs. The Brueckner-Hartree-Fock (BHF) approximation for the single-particle potential $U(k;\rho)$ using the continuous choice is

$$U(k;\rho)=\mathrm{Re}\sum_{k'<k_F}\langle kk'|G[\rho;e(k)+e(k')]|kk'\rangle_a, \tag{3}$$

where the subscript "a" indicates antisymmetrization of the matrix element. Due to the occurrence of $U(k)$ in Eq. (2), they constitute a coupled system that has to be solved in a self-consistent manner for several Fermi momenta of the particles involved. In the BHF approximation the energy per nucleon is

$$\frac{E}{A}=\frac{3}{5}\frac{k_F^2}{2m}+\frac{1}{2\rho}\sum_{k,k'<k_F}\langle kk'|G[\rho;e(k)+e(k')]|kk'\rangle_a. \tag{4}$$

In this scheme, the only input quantity we need is the bare NN interaction v in the Bethe-Goldstone equation (1). In this sense the BBG approach can be considered as a microscopic one. The nuclear EOS can be calculated with good accuracy in the Brueckner two hole-line approximation with the continuous choice for the single-particle potential, since the results in this scheme are quite close to the calculations which include also the three hole-line contribution [7]. In the calculations reported here, we have used the Argonne v_{18} potential [8] as the two-nucleon interaction.

However, it is commonly known that nonrelativistic calculations, based on purely two-body interactions, fail to reproduce the correct saturation point of symmetric nuclear matter, and three-body forces (TBF) among nucleons are needed to correct this deficiency. In this work the so-called Urbana model will be used, which consists of an attractive term due to two-pion exchange with excitation of an intermediate Δ resonance, and a repulsive phenomenological central term [9]. We introduced the same Urbana three-nucleon model within the BHF approach (for more details see Ref. [3]). In our approach the TBF is reduced to a density dependent two-body force by averaging over the position of the third particle, assuming that the probability of having two particles at a given distance is reduced according to the two-body correlation function determined self-consistently. The corresponding nuclear matter EOS fulfills several requirements, namely (i) it reproduces the correct nuclear matter saturation point, (ii) the incompressibility is compatible with the values extracted from phenomenology, (iii) the symmetry energy is compatible with nuclear phenomenology, (iv) the causality condition is always fulfilled.

In order to study the structure of neutron stars, we have to calculate the composition and the EOS of cold, neutrino-free, catalyzed matter. We require that the neutron star contains charge neutral matter consisting of neutrons, protons, and leptons (e^-, μ^-) in beta equilibrium, and compute the EOS for charge neutral and beta-stable matter in the following standard way [2,3,10]: The Brueckner calculation yields the energy density of lepton/baryon matter as a function of the different partial densities,

$$\begin{aligned}\epsilon(\rho_n,\rho_p,\rho_e,\rho_\mu)&=(\rho_n m_n+\rho_p m_p)+(\rho_n+\rho_p)\frac{E}{A}(\rho_n,\rho_p)\\&\quad+\rho_\mu m_\mu+\frac{1}{2m_\mu}\frac{(3\pi^2\rho_\mu)^{5/3}}{5\pi^2}\\&\quad+\frac{(3\pi^2\rho_e)^{4/3}}{4\pi^2},\end{aligned} \tag{5}$$

where we have used ultrarelativistic and nonrelativistic approximations for the energy densities of electrons and muons, respectively. In practice, it is sufficient to compute only the binding energy of symmetric nuclear matter and pure neutron matter, since within the BHF approach it has been verified [11,12] that a parabolic approximation for the binding energy of nuclear matter with arbitrary proton fraction $x=\rho_p/\rho$, $\rho=\rho_n+\rho_p$, is well fulfilled,

$$\frac{E}{A}(\rho,x)\approx\frac{E}{A}(\rho,x=0.5)+(1-2x)^2E_{\mathrm{sym}}(\rho), \tag{6}$$

where the symmetry energy E_{sym} can be expressed in terms of the difference of the energy per particle between pure neutron ($x=0$) and symmetric ($x=0.5$) matter:

$$E_{\mathrm{sym}}(\rho)=-\frac{1}{4}\frac{\partial(E/A)}{\partial x}(\rho,0)\approx\frac{E}{A}(\rho,0)-\frac{E}{A}(\rho,0.5). \tag{7}$$

Knowing the energy density Eq. (5), the various chemical potentials (of the species $i=n,p,e,\mu$) can be computed straightforwardly,

$$\mu_i=\frac{\partial\epsilon}{\partial\rho_i}, \tag{8}$$

and the equations for beta-equilibrium,

$$\mu_i=b_i\mu_n-q_i\mu_e, \tag{9}$$

(b_i and q_i denoting baryon number and charge of species i) and charge neutrality,

$$\sum_i\rho_i q_i=0, \tag{10}$$

allow one to determine the equilibrium composition $\rho_i(\rho)$ at given baryon density ρ and finally the EOS,

$$P(\rho)=\rho^2\frac{d}{d\rho}\frac{\epsilon(\rho_i(\rho))}{\rho}=\rho\frac{d\epsilon}{d\rho}-\epsilon=\rho\mu_n-\epsilon. \tag{11}$$

B. Hyperons in nuclear matter

While at moderate densities $\rho \approx \rho_0$ the matter inside a neutron star consists only of nucleons and leptons, at higher densities several other species of particles may appear due to the fast rise of the baryon chemical potentials with density. Among these new particles are strange baryons, namely, the Λ, Σ, and Ξ hyperons. Due to its negative charge, the Σ^- hyperon is the first strange baryon expected to appear with increasing density in the reaction $n+n \rightarrow p+\Sigma^-$, in spite of its substantially larger mass compared to the neutral Λ hyperon ($M_{\Sigma^-}=1197$ MeV, $M_\Lambda=1116$ MeV). Other species might appear in stellar matter, like Δ isobars along with pion and kaon condensates. It is therefore mandatory to generalize the study of the nuclear EOS with the inclusion of the possible hadrons, other than nucleons, which can spontaneously appear in the inner part of a neutron star, just because their appearance is able to lower the ground state energy of the dense nuclear matter phase.

As we have pointed out in the previous section, the nuclear EOS can be calculated with good accuracy in the Brueckner two hole-line approximation with the continuous choice for the single-particle potential, since the results in this scheme are quite close to the full convergent calculations which include also the three hole-line contribution. It is then natural to include the hyperon degrees of freedom within the same approximation to calculate the nuclear EOS needed to describe the neutron star interior. To this purpose, one requires in principle nucleon-hyperon (*NY*) and hyperon-hyperon (*YY*) potentials. In our work we use the Nijmegen soft-core *NY* potential [13] that is well adapted to the available experimental *NY* scattering data. Unfortunately, to date no *YY* scattering data and therefore no reliable *YY* potentials are available. We therefore neglect these interactions in our calculations, which is supposedly justified, as long as the hyperonic partial densities remain limited. Also, for the following calculations the v_{18} *NN* potential together with the phenomenological *TBF* introduced previously, are used.

With the *NN* and *NY* potentials, the various *G* matrices are evaluated by solving numerically the Brueckner equation, which can be written in operatorial form as [11,14]

$$G_{ab}[W]=V_{ab}+\sum_c \sum_{p,p'} V_{ac}|pp'\rangle \frac{Q_c}{W-E_c+i\epsilon} \times \langle pp'|G_{cb}[W], \tag{12}$$

where the indices a,b,c indicate pairs of baryons and the Pauli operator Q and energy E determine the propagation of intermediate baryon pairs. In a given nucleon-hyperon channel $c=(NY)$ one has, for example,

$$E_{(NY)}=m_N+m_Y+\frac{k_N^2}{2m_N}+\frac{k_Y^2}{2m_Y}+U_N(k_N)+U_Y(k_Y). \tag{13}$$

The hyperon single-particle potentials within the continuous choice are given by

$$U_Y(k)=\mathrm{Re}\sum_{N=n,p}\sum_{k'<k_F^{(N)}}\langle kk'|G_{(NY)(NY)}[E_{(NY)}(k,k')]|kk'\rangle \tag{14}$$

and similar expressions of the form

$$U_N(k)=\sum_{N'=n,p}U_N^{(N')}(k)+\sum_{Y=\Sigma^-,\Lambda}U_N^{(Y)}(k) \tag{15}$$

apply to the nucleon single-particle potentials. The nucleons feel therefore direct effects of the other nucleons as well as of the hyperons in the environment, whereas for the hyperons there are only nucleonic contributions, because of the missing hyperon-hyperon potentials. Equations (12)–(15) define the BHF scheme with the continuous choice of the single-particle energies. In contrast to the standard purely nucleonic calculation there is now an additional coupled channel structure, which renders a self-consistent calculation quite time-consuming.

Once the different single-particle potentials are known, the total nonrelativistic baryonic energy density, ϵ, can be evaluated:

$$\epsilon=\sum_{i=n,p,\Sigma^-,\Lambda}\int_0^{k_F^{(i)}}\frac{dkk^2}{\pi^2}\left[m_i+\frac{k^2}{2m_i}+\frac{1}{2}U_i(k)\right] \tag{16}$$

$$=\epsilon_{NN}+\sum_{Y=\Sigma^-,\Lambda}\int_0^{k_F^{(Y)}}\frac{dkk^2}{\pi^2}\left[m_Y+\frac{k^2}{2m_Y}+U_Y^{(n)}(k)+U_Y^{(p)}(k)\right], \tag{17}$$

where ϵ_{NN} is the nucleonic part of the energy density, Eq. (5). Using for example an effective mass approximation for the hyperon single-particle potentials, one could write the last term due to the nucleon-hyperon interaction as

$$\epsilon_{NY}=\sum_{Y=\Sigma^-,\Lambda}\left(\rho_Y[m_Y+U_Y(0)]+\frac{1}{2m_Y^*}\frac{(3\pi^2\rho_Y)^{5/3}}{5\pi^2}\right), \tag{18}$$

which should be added to Eq. (5).

The knowledge of the energy density allows one then to compute EOS and neutron star structure as described before, now making allowance for the species $i=n,p,\Sigma^-,\Lambda,e^-,\mu^-$. The main physical features of the nuclear EOS which determine the resulting compositions are essentially the symmetry energy of the nucleon part of the EOS and the hyperon single-particle potentials inside nuclear matter. Since at low enough density the nucleon matter is quite asymmetric, the small percentage of protons feel a deep single-particle potential, and therefore it is energetically convenient to create a Σ^- hyperon, since then a neutron can be converted into a proton. The depth of the proton potential is mainly determined by the nuclear matter symmetry energy. Furthermore, the potentials felt by the hyperons can shift substantially the threshold density at which each hyperon sets in.

We have found rather low hyperon onset densities of about 2 to 3 times normal nuclear matter density for the appearance of the Σ^- and Λ hyperons [11]. (Other hyperons do not appear in the matter.) Moreover, an almost equal percentage of nucleons and hyperons are present in the stellar core at high densities. The inclusion of hyperons produces an EOS which turns out to be much softer than the purely nucleonic case. The consequences for the structure of the neutron stars are dramatic. In fact the presence of hyperons leads to a maximum mass for neutron stars of less than 1.3 solar masses [11], which is below the observational limit.

This surprising result is due to the strong softening of the baryonic EOS when including hyperons as additional degrees of freedom. We do not expect substantial changes when introducing refinements of the theoretical framework, such as hyperon-hyperon potentials [15], relativistic corrections, etc. Three-body forces involving hyperons could produce a substantial stiffening of the baryonic EOS. Unfortunately they are essentially unknown, but can be expected to be weaker than in the non-strange sector. Another possibility that is able to produce larger maximum masses is the appearance of a transition to another phase of dense (quark) matter inside the star. This will be discussed in the following.

III. QUARK PHASE

The results obtained with a purely baryonic EOS call for an estimate of the effects due to the hypothetical presence of quark matter in the interior of the neutron star. Unfortunately, the current theoretical description of quark matter is burdened with large uncertainties, seriously limiting the predictive power of any theoretical approach at high baryonic density. For the time being we can therefore only resort to phenomenological models for the quark matter EOS and try to constrain them as well as possible by the few experimental information on high density baryonic matter.

One of these constraints is the phenomenological observation that in heavy ion collisions at intermediate energies ($10\ \mathrm{MeV}/A \lesssim E/A \lesssim 200\ \mathrm{MeV}/A$) no evidence for a transition to a quark-gluon plasma has been found. Indeed, all microscopic simulations, like BUU or QMD, that are able to reproduce a great variety of experimental data, do not need the introduction of such a transition [16]. In these simulations the calculated nucleon density can reach values which are at least 2 to 3 times larger than the saturation density ρ_0. One can, therefore, conclude that symmetric or nearly symmetric nuclear matter at a few MeV of temperature does not exhibit any phase transition to deconfined matter up to this baryon density. It has to be noticed that the phase transition in symmetric matter can occur at a substantially different baryon density than in neutron star matter, where nuclear matter is closer to neutron matter than to symmetric nuclear matter.

This constraint coming from heavy-ion physics appears as an independent one, that should be fulfilled by any theory or model of deconfinement. Indeed, quark matter models can have, in some cases, serious difficulties to fulfill the constraint (the transition occurring at too low density), even if they produce ''reasonable'' results for neutron stars, where the transition does occur. We will in the following take this constraint in due consideration, and use an extended MIT bag model [17] (including the possibility of a density dependent bag ''constant'') and the color dielectric model [18], both compatible with this condition.

A. The MIT bag model

We first review briefly the description of the bulk properties of uniform quark matter, deconfined from the β-stable hadronic matter mentioned in the previous section, by using the MIT bag model [17]. The thermodynamic potential of $f=u,d,s$ quarks can be expressed as a sum of the kinetic term and the one-gluon-exchange term [19,20] proportional to the QCD fine structure constant α_s,

$$\Omega_f(\mu_f) = -\frac{3m_f^4}{8\pi^2}\left[\frac{y_f x_f}{3}(2x_f^2-3)+\ln(x_f+y_f)\right] + \alpha_s\frac{3m_f^4}{2\pi^3}\left\{[y_f x_f-\ln(x_f+y_f)]^2-\frac{2}{3}x_f^4+\ln(y_f) + 2\ln\left(\frac{\sigma_{\mathrm{ren}}}{m_f y_f}\right)[y_f x_f-\ln(x_f+y_f)]\right\}, \tag{19}$$

where m_f and μ_f are the f current quark mass and chemical potential, respectively, $y_f=\mu_f/m_f$, $x_f=\sqrt{y_f^2-1}$, and $\sigma_{\mathrm{ren}}=313$ MeV is the renormalization point. In this work we will consider massless u and d quarks (together with $m_s=150$ MeV), in which case the above expression reduces to

$$\Omega_q = -\frac{\mu_q^4}{4\pi^2}\left(1-\frac{2\alpha_s}{\pi}\right) \quad (q=u,d). \tag{20}$$

The number density ρ_f of f quarks is related to Ω_f via

$$\rho_f = -\frac{\partial\Omega_f}{\partial\mu_f}, \tag{21}$$

and the total energy density for the quark system is written as

$$\epsilon_{\mathrm{MIT}}(\rho_u,\rho_d,\rho_s) = \sum_f\ (\Omega_f+\mu_f\rho_f)+B, \tag{22}$$

where B is the energy density difference between the perturbative vacuum and the true vacuum, i.e., the bag ''constant.'' In the original MIT bag model $B\approx 55\ \mathrm{MeV\ fm^{-3}}$ is used, while values $B\approx 210\ \mathrm{MeV\ fm^{-3}}$ are estimated from lattice calculations [21]. In this sense B can be considered as a free parameter.

The composition of β-stable quark matter is determined by imposing the condition of equilibrium under weak interactions for the following processes:

$$u + e^- \to d + \nu_e, \tag{23a}$$

$$u + e^- \to s + \nu_e, \tag{23b}$$

$$d \to u + e^- + \bar{\nu}_e, \tag{23c}$$

$$s \to u + e^- + \bar{\nu}_e, \tag{23d}$$

$$s + u \to d + u. \tag{23e}$$

In neutrino-free matter ($\mu_{\nu_e} = \mu_{\bar{\nu}_e} = 0$), the above equations imply for the chemical potentials

$$\mu_d = \mu_s = \mu_u + \mu_e. \tag{24}$$

As in baryonic matter, the relations for chemical equilibrium must be supplemented with the charge neutrality condition and the total baryon number conservation,

$$0 = \frac{1}{3}(2\rho_u - \rho_d - \rho_s) - \rho_e, \tag{25}$$

$$\rho = \frac{1}{3}(\rho_u + \rho_d + \rho_s), \tag{26}$$

in order to determine the composition $\rho_f(\rho)$ and the pressure of the quark phase,

$$P_Q(\rho) = \rho \frac{d\epsilon_Q}{d\rho} - \epsilon_Q. \tag{27}$$

It has been found [22,23] that within the MIT bag model (without color superconductivity) with a density independent bag constant B, the maximum mass of a NS cannot exceed a value of about 1.6 solar masses. Indeed, the maximum mass increases as the value of B decreases, but too small values of B are incompatible with a transition density $\rho > (2, \ldots, 3)\rho_0$ in symmetric nuclear matter, as demanded by heavy-ion collision phenomenology according to the preceding discussion. In order to avoid this serious drawback of the model, one can introduce a density-dependent bag "constant" $B(\rho)$, and this approach was followed in Ref. [23]. This allows one to lower the value of B at large density, providing a stiffer quark matter EOS and increasing the value of the maximum mass, while at the same time still fulfilling the condition of no phase transition below $\rho \approx 3\rho_0$. The comparison of the predictions based on the MIT bag model and the CDM can be considered meaningful only if this constraint is maintained also in the CDM. One has to keep in mind that the constraint is meant for symmetric nuclear matter. Its influence on the results for NS is related to the density dependent value of the symmetry energy, which is an intrinsic characteristic of the model.

In the following we present results based on the MIT model using a constant value of the bag constant, $B = 90$ MeV/fm^3, and a Gaussian parametrization for the density dependence,

$$B(\rho) = B_\infty + (B_0 - B_\infty)\exp\left[-\beta\left(\frac{\rho}{\rho_0}\right)^2\right] \tag{28}$$

with $B_\infty = 50$ MeV fm^{-3}, $B_0 = 400$ MeV fm^{-3}, and $\beta = 0.17$. As discussed later (Sec. IV A), the results on the maximum mass depend only marginally on the particular parametrization adopted for B(ρ). As for the value of α_s, all the results shown in this paper have been obtained choosing $\alpha_s = 0$, but we have checked that they are not very sensitive to the value of α_s [23].

B. The color dielectric model

Let us now consider the color dielectric model, which was originally introduced [18] as a confinement model of the nucleon (see the general reviews [24–26]). In the CDM the nucleon is described as a soliton in which quarks are dynamically confined via the interaction with a scalar-isoscalar chiral singlet field, indicated in the following as χ, whose quanta correspond to glueballs or hybrid mesons. Several closely related versions of the CDM exist in the literature. They have been widely employed in the baryon sector, to calculate the static [27–30] and dynamic properties [31–36] of the nucleon and to describe strange baryons [28,37–39]. The CDM has also been applied in the quark sector, to calculate the EOS of quark matter [40–44] and to study the stability of strange quark matter [45]. Applications of the CDM EOS for quark matter to the study of compact stars have been considered by Ghosh *et al.* [46] and by Drago and collaborators, who studied the structure of hybrid stars [47,48] and the problem of supernova explosions [49], and, more recently by Malheiro *et al.* [50,51] to study pure quark stars.

In this work we use the chiral version of the CDM [41,44], extended to include strange quarks [40,47], which, as shown in Ref. [44], describes reasonably well the nucleon, while giving, with the same set of parameter values, a meaningful equation of state for symmetric quark matter. The Lagrangian of the model reads

$$\begin{aligned}\mathcal{L} = &\sum_{f=u,d,s} i\bar{\psi}_f \gamma^\mu \partial_\mu \psi_f + \sum_{f=u,d} \frac{g_f}{f_\pi \chi}\bar{\psi}_f(\sigma + i\boldsymbol{\tau}\cdot\boldsymbol{\pi}\gamma_5)\psi_f \\ &- \frac{g_s}{\chi}\bar{\psi}_s\psi_s + \frac{1}{2}(\partial_\mu\sigma)^2 + \frac{1}{2}(\partial_\mu\boldsymbol{\pi})^2 - U(\sigma,\boldsymbol{\pi}) + \frac{1}{2}(\partial_\mu\chi)^2 \\ &- V(\chi).\end{aligned} \tag{29}$$

Here the potential $V(\chi)$ has the quadratic form

$$V(\chi) = \frac{1}{2}M^2\chi^2, \tag{30}$$

while

$$U(\sigma,\boldsymbol{\pi}) = \frac{m_\sigma^2}{8f_\pi^2}(\sigma^2 + \boldsymbol{\pi}^2 - f_\pi^2)^2 \tag{31}$$

is the usual ''Mexican hat'' potential. The characteristic feature of the CDM is the coupling of the quarks to an inverse power of the field χ, through which the quarks acquire density dependent effective masses $m_{u,d}=-g_{u,d}\sigma/f_\pi\chi$ and $m_s=g_s/\chi$. Since χ vanishes in the vacuum, the quark masses diverge as the density ρ goes to zero, thus providing confinement.

In Eq. (29) the couplings are given by $g_{u,d}=g(f_\pi\pm\xi_3)$ and $g_s=g(2f_K-f_\pi)$, where $f_\pi=93$ MeV and $f_K=113$ MeV are the pion and the kaon decay constants, respectively, and where $\xi_3=f_{K^\pm}-f_{K^0}=-0.75$ MeV. In Eq. (31) we take $m_\sigma=1.2$ GeV.

The parameters of the model are thus g, determining the couplings g_f, and the mass M of the χ field. At the mean field level, and with the form Eq. (30) of the potential, the only free parameter is actually the product $G=\sqrt{gM}$. In the following we will use the values $M=1.7$ GeV and $g=23$ MeV (corresponding to $G=198$ MeV), which were obtained in Ref. [47], by requiring that the model provides reasonable values for the average delta-nucleon mass and for the nucleon isoscalar radius.

To describe the possible quark phase in the interior of a neutron star we consider a uniform system of plane wave u, d, and s quarks interacting with the fields χ and σ. In the mean field approximation the latter are assumed to be constant, while the pion field vanishes. The energy density of the system is then given by

$$\epsilon_{\rm CDM}=\gamma\sum_{f=u,d,s}\sum_{k<k_F^f}\sqrt{\boldsymbol{k}^2+m_f(\sigma,\chi)^2}+V(\chi)+U(\sigma,\boldsymbol{\pi}=\mathbf{0}), \tag{32}$$

where $\gamma=6$ is the spin and color degeneracy factor and k_F^f are the Fermi momenta of the quarks of flavor f. At fixed baryon density, two coupled equations for the fields χ and σ are obtained by minimizing the energy density $\epsilon_{\rm CDM}$:

$$\frac{dV(\chi)}{d\chi}=-\sum_{f=u,d}\rho_S^f(k_F^f,m_f)\frac{g_f\sigma}{f_\pi\chi^2}+\rho_S^s(k_F^s,m_s)\frac{g_s}{\chi^2}, \tag{33}$$

$$\frac{dU(\sigma,\mathbf{0})}{d\sigma}=\sum_{f=u,d}\rho_S^f(k_F^f,m_f)\frac{g_f}{f_\pi\chi}, \tag{34}$$

where

$$\rho_S^f(k_F^f,m_f)=\gamma\sum_{k<k_F^f}\frac{m_f}{\sqrt{\boldsymbol{k}^2+m_f^2}} \tag{35}$$

are the quark scalar densities. By imposing chemical equilibrium, supplemented by the conditions of charge neutrality and baryon number conservation, Eqs. (24)–(26) along with Eqs. (33)–(35) form a system of six coupled equations, which are solved self-consistently to get $\chi,\sigma,k_F^u,k_F^d,k_F^s$, and k_F^e. Once they are solved, we obtain the population of each quark flavor $\rho_f=\gamma(k_F^f)^3/6\pi^2$, as well as the one of the electrons.

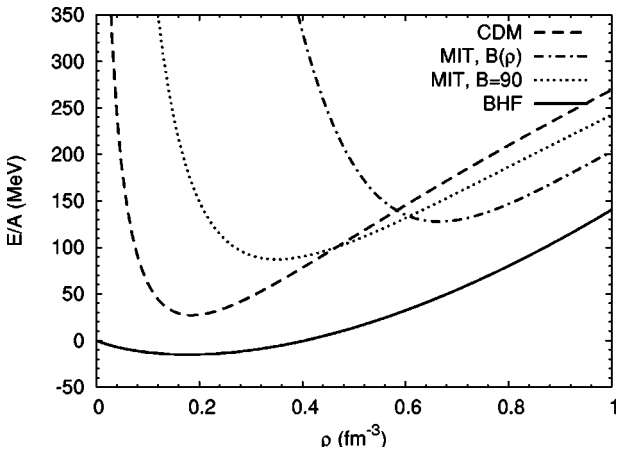

FIG. 1. Energy per baryon for symmetric matter calculated for the purely nucleonic case (solid line), with the MIT bag models (dotted and dot-dashed lines), and with the CDM (dashed line).

IV. RESULTS AND DISCUSSION

A. Phase transition in symmetric matter

Before studying the quark phase inside neutron stars, let us first discuss the EOS of symmetric matter. We calculate the EOS for cold symmetric nuclear matter in the BHF formalism with two-body and three-body forces, as described above in Sec. II. Then we calculate the EOS for u and d quark matter, using, respectively, Eq. (22) for the MIT bag model and Eq. (32) for the CDM. The results are displayed in Fig. 1. The solid line represents the purely nucleonic case within the Brueckner many-body approach, whereas the different broken lines denote the results for the various quark matter EOS. We find that, in the range of baryon densities explored, the quark matter energy is always higher than that of symmetric nuclear matter, independent of the model adopted for describing the quark phase. Therefore nuclear matter is the favorite state.

As far as the results obtained with the MIT bag model are concerned, some clarification is needed. In fact, apart from a bag constant $B=90$ MeV fm^{-3}, we have also used a density dependent bag parameter $B(\rho)$, whose parametrization is the one of Eq. (28). This was adopted in previous works [23], and we repeat here briefly the motivations. The condition of no quark transition in symmetric nuclear matter below $(3,\ldots,4)\rho_0$ constrains the low density behavior of $B(\rho)$, whereas at high density a further constraint is needed. The value of $B(\rho)$ was then assumed to decrease fast enough so that a transition to quark matter could occur at a density compatible with the one extracted from CERN SPS data [52], i.e., $\rho_c\approx 6\rho_0\approx 1/\text{fm}^3$. This value was estimated by assuming that the transition is determined by the value of the energy density along the transition line in the pressure-chemical potential plane, as now indeed recent lattice calculations seem to indicate [53]. Of course this condition does

not fix completely the behavior of $B(\rho)$, but it turns out [23] that the results for the NS maximum mass are only marginally affected by the precise trend of $B(\rho)$.

As discussed above, in the present calculations, which are updating the EOS used in Ref. [23], no transition actually occurs in symmetric matter, even if quark and hadronic matter are almost overlapping at high density near ρ_c. However, at higher baryonic density the precise trend of the EOS of symmetric hadronic matter is surely more uncertain. A refinement of the EOS could lead to a transition to a deconfined phase at a higher baryonic density, compatible with this value of ρ_c. In particular, different sets of three-body forces and the inclusion of three hole-line diagrams can produce indeed a stiffening of the hadronic EOS and the transition to quark matter can occur at this high density. A critical discussion on this point will be published elsewhere. In any case, these refinements do not affect the results in NS matter, since there, due to the appearance of hyperons and quark matter, the purely hadronic phase never reaches a density higher than $(3,\ldots,4)\rho_0$, and the uncertainty in the high density EOS of nuclear matter plays no role.

In order to facilitate the comparison between the different quark models adopted in this work, it is useful to introduce in the CDM an effective bag parameter, which describes the difference between the quark matter energy density and the energy density of a system of free quarks of fixed mass m_f' having the same density and composition. We thus define

$$B_{\rm eff}(\rho) \equiv \epsilon_{\rm CDM} - \gamma \sum_{f=u,d,s} \sum_{k<k_F^f} \sqrt{\boldsymbol{k}^2 + m_f'^2}, \qquad (36)$$

where we take $m_u' = m_d' = 0$, $m_s' = 150$ MeV in order to compare with the bag parameter used in the MIT model. As an alternative [54], one can also define a bag parameter as the ''non-quark'' contribution to the energy density,

$$B_{\rm eff}'(\rho) \equiv \epsilon_{\rm CDM} - \gamma \sum_{f=u,d,s} \sum_{k<k_F^f} \sqrt{\boldsymbol{k}^2 + m_f(\sigma,\chi)^2} \qquad (37)$$

$$= V(\chi) + U(\sigma, \boldsymbol{\pi} = \boldsymbol{0}). \qquad (38)$$

The effective bag parameters $B_{\rm eff}$ and $B_{\rm eff}'$ are plotted versus the baryon density ρ in Fig. 2 for symmetric matter. We observe that, although at low baryon density the bag parameters used with the MIT model are larger than the one calculated with the CDM, asymptotically they all reach values in the range $(50,\ldots,120)$ MeV fm^{-3}. However, in the former case the effective bag constant is a monotonically decreasing function of the density, at variance with the CDM and also with the Nambu-Jona-Lasinio model, widely studied in Refs. [54,55].

B. Phase transition in asymmetric β-stable matter

We now consider the hadron-quark phase transition in neutron stars, and calculate the EOS of a conventional neutron star as composed of a chemically equilibrated and charge neutral mixture of nucleons, hyperons, and leptons. The result is tabulated in Table I and shown by the solid line in Fig. 3(a). The dashed line represents the EOS of beta-stable and charge neutral (u,d,s) quark matter obtained within the CDM, and the dotted and dot-dashed lines the results due to the MIT model with constant and density dependent B, respectively. Markers indicate the crossing points between the hadron and the quark phases. We notice that the crossing from hadronic to quark matter occurs at very low baryonic density when the CDM is used to describe the quark phase, whereas higher values of the transition density are predicted with the MIT bag model. In fact, the density dependent bag parameter was introduced in order to shift this transition to high density and to explore the implications for the NS observables.

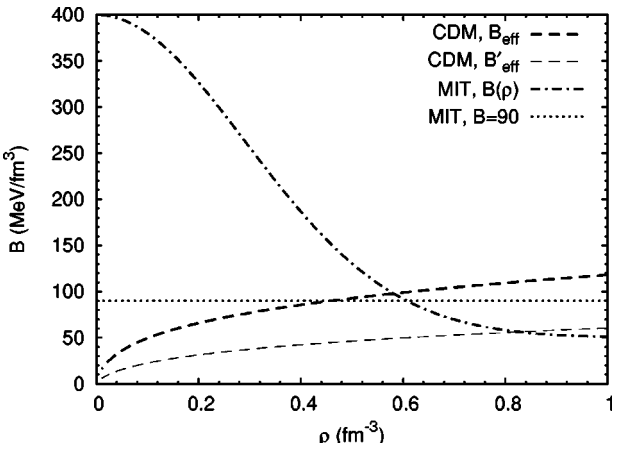

FIG. 2. The bag parameters B are shown as function of the baryon density for symmetric matter. The dot-dashed line shows the parametrization Eq. (28) used in the MIT model, whereas the dashed lines represent the effective values of the CDM, calculated using Eqs. (36) or Eq. (38), respectively.

A more realistic model for the phase transition between baryonic and quark phase inside the star is the Glendenning construction [2,56], which determines the range of baryon density where both phases coexist, yielding an EOS contain-

TABLE I. Baryonic EOS used in our calculations.

ρ_B [fm^{-3}]	ϵ [MeV/fm^3]	P [MeV/fm^3]	$\mu_B - m_N$ [MeV]
0.1	94.8	0.97	18.2
0.2	192	5.2	46.0
0.3	292	15.3	86.0
0.4	397	26.7	115
0.5	504	39.7	143
0.6	615	54.8	168
0.7	728	72.0	192
0.8	843	91.0	215
0.9	962	112	236
1.0	1082	135	256
1.1	1205	159	275
1.2	1330	185	293
1.3	1458	213	311
1.4	1587	242	328
1.5	1719	273	344

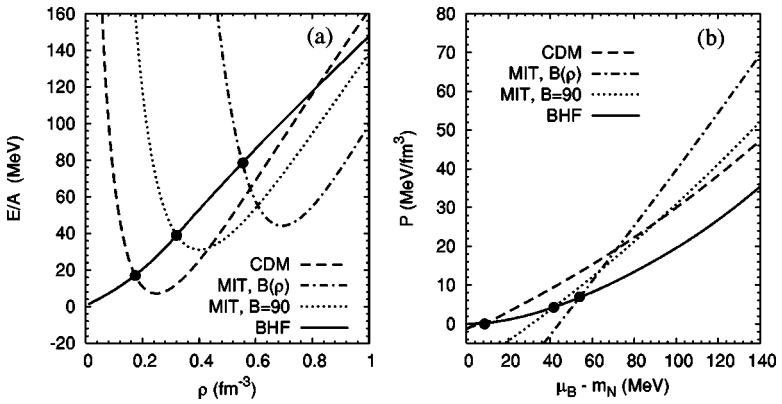

FIG. 3. Panel (a) displays the energy per particle vs baryon density for beta-stable matter in the BHF approach (solid line) and for u,d,s quark matter obtained within the MIT model (dotted and dot-dashed lines) and the CDM (dashed line). Panel (b) shows the pressure as function of the baryonic chemical potential for all cases.

ing a pure hadron phase, a mixed phase, and a pure quark matter region. In our previous papers [23], we have used the Glendenning construction, demonstrating that in particular the influence on the maximum mass value is rather small. Apart from that, the realization of the mixed phase depends on the nuclear surface tension, which is currently an unknown parameter. In fact, even a relatively small surface tension seems to disfavor a mixed phase [57].

Therefore, in the present work we adopt the simpler Maxwell construction. For that, we construct the phase transition from Fig. 3(b), showing the pressure as a function of the baryonic chemical potential μ_B. The transition is determined by the intersection points between the hadronic (solid line) and the different quark phases. We notice that the phase transition occurs at very low values of the baryon density, $\rho \approx 0.05$ fm^{-3}, when the CDM is used. The transition density that we obtain is somewhat lower than the value obtained in Ref. [47], where, using the Walecka model to describe the hadronic EOS, a mixed phase was found to occur in the interval 0.1 fm$^{-3} \leqslant \rho \leqslant 0.31$ fm^{-3}. However, the general result that the pure quark phase starts at a rather low density is in agreement with Ref. [47].

The phase transition constructed with the CDM and the corresponding neutron star structure are quite different from the ones obtained using the MIT bag model. In the CDM the onset of the quark phase occurs at very low density, and the pure deconfined phase occupies most of the star. This picture is expected still to hold if, instead of a sharp phase transition, a mixed phase is allowed. In the MIT bag model the pure quark phase is still the dominant component of the star, at least for the higher masses, but a well developed hadronic phase is present in the lower density region. This pure hadronic component still persists if the mixed phase is introduced [23]. The scenario is again different within the Nambu-Jona-Lasinio model [55], where at most a mixed phase could be present, but no pure quark phase.

As a peculiarity, we mention that at high density ($\rho \approx 0.93$ fm^{-3}) within the CDM a second crossing in the $p-\mu$ plane occurs. This looks disturbing, since it seems unlikely that at so high density baryonic matter could appear again. This feature could be attributed to the hyperonic component of the hadronic phase, since no second crossing is present if only nucleons are considered. However, the strength of the softening depends on the extrapolation of the adopted hyperon-nucleon interaction to high density, where no phenomenological input is available. The behavior of the quark EOS in the CDM also plays a role, since the second crossing does not occur in the MIT bag model, at least in the density range relevant for NS calculations.

In any case the physical picture of distinct quark and baryonic phases at such high density is doubtful. In the calculations we have therefore ignored this second crossing and followed the quark branch. It has to be stressed that the transition from hadronic to quark matter at low density occurs before the appearance of hyperons, so that the use of an only nucleonic (no hyperon) EOS would yield the same results for the CDM.

C. Neutron star structure

We assume that a neutron star is a spherically symmetric distribution of mass in hydrostatic equilibrium. The equilibrium configurations are obtained by solving the Tolman-Oppenheimer-Volkoff (TOV) equations [10] for the pressure P and the enclosed mass m,

$$\frac{dP(r)}{dr} = -\frac{Gm(r)\epsilon(r)}{r^2} \times \frac{[1+P(r)/\epsilon(r)][1+4\pi r^3 P(r)/m(r)]}{1-2Gm(r)/r}, \tag{39}$$

$$\frac{dm(r)}{dr} = 4\pi r^2 \epsilon(r), \tag{40}$$

G being the gravitational constant. Starting with a central mass density $\epsilon(r=0) \equiv \epsilon_c$, we integrate out until the pressure on the surface equals the one corresponding to the density of iron. This gives the stellar radius R and the gravitational mass is then

$$M_G \equiv m(R) = 4\pi \int_0^R dr r^2 \epsilon(r). \tag{41}$$

We have used as input the equations of state discussed above for the CDM and the MIT bag model for the beta-stable quark phase, and the BHF for the hadronic matter. For the

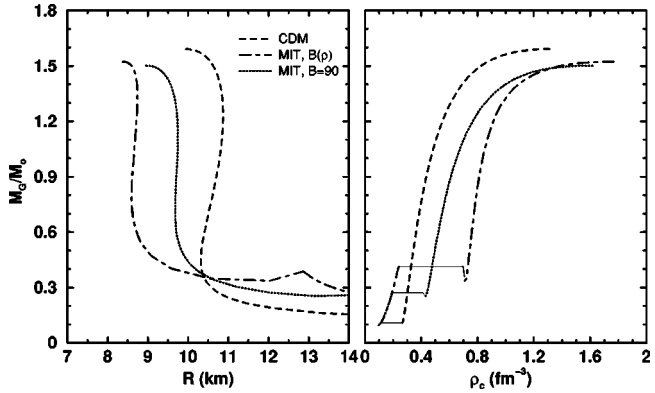

FIG. 4. The mass (in units of solar mass $M_\odot = 1.98 \times 10^{33}$ g) is displayed as function of radius (left panel) and central density (right panel), using different EOS. See the text for details.

description of the NS crust, we have joined the hadronic EOS with the ones by Negele and Vautherin [58] in the medium-density regime, and the ones by Feynman-Metropolis-Teller [59] and Baym-Pethick-Sutherland [60] for the outer crust.

The results are plotted in Fig. 4, where we display the gravitational mass M_G (in units of the solar mass $M_\odot$) as a function of the radius R (left panel) and central baryon density ρ_c (right panel). The dashed lines represent the calculation for beta-stable quark matter with the CDM, whereas the dotted and dot-dashed lines denote the results obtained with the MIT bag model. Due to the use of the Maxwell construction, the mass – central density curves are not continuous [2]: For very small central densities (large radii, small masses) the stars are purely hadronic. Then a sudden increase of the central density is required in order to start the quark phase in the center of the star, corresponding to the phase diagram Fig. 3(b). By performing the Glendenning construction, the curves would become continuous.

We have also observed at the onset of quark matter a sort of cusp in the mass vs radius plot, left panel of Fig. 4, in the very low mass region and large radius. This corresponds to the ''wiggle'' in the plot of mass vs central density, right panel of Fig. 4. This turns out to be typical in the calculation with a sharp phase transition, see, e.g., Ref. [2]. This also implies a small region where the NS is unstable. In any case, with our EOS the relevant mass values are quite small and do not correspond to physical neutron stars.

We observe that the values of the maximum mass depend only slightly on the EOS chosen for describing quark matter, and lie between 1.5 and 1.6 solar masses. A clear difference between the two models exists as far as the radius is concerned. Hybrid stars built with the CDM are characterized by a larger radius and a smaller central density, whereas hybrid stars constructed with the MIT bag model are more compact, since they contain quark matter of higher density.

This is also illustrated in Fig. 5, showing the different internal structure of stars with the MIT model and the CDM by comparing the populations of quarks and baryons inside a $M = 1.4 M_\odot$ neutron star. At this value of the mass, within the MIT model only a thin hadronic layer is present, mainly composed of neutrons, followed by a small portion of crust,

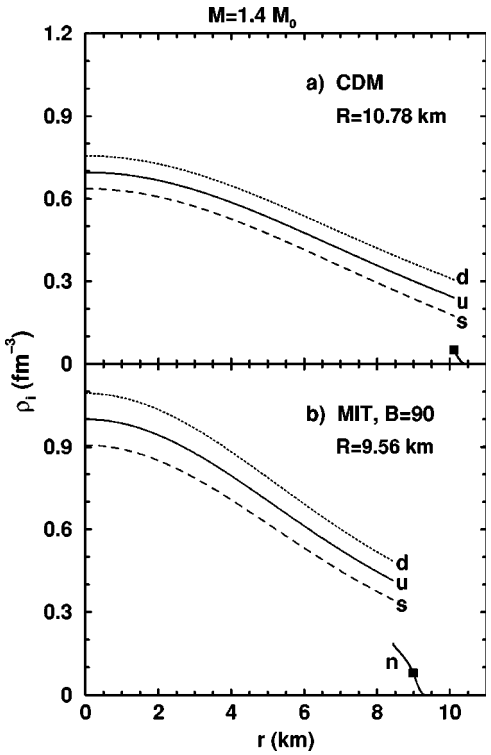

FIG. 5. The particle populations inside a $M = 1.4 M_\odot$ neutron star with the CDM (upper panel) and the bag model (lower panel) quark matter EOS. The markers indicate the beginning of the crust.

whereas in the case of the CDM one finds only crustal matter. The central (quark) density is substantially larger with the MIT model, in agreement with Fig. 4. In both models, the abrupt transition from quark to hadronic matter is a consequence of the Maxwell construction.

V. CONCLUSIONS

In this article we determine the structure of neutron stars, combining the most recent microscopic baryonic EOS in the BHF approach involving three-body forces and hyperons with different effective models describing the quark matter phase.

Without allowing for the presence of quark matter, the maximum neutron star mass remains below 1.3 solar masses, due to the strong softening effect of the hyperons on the EOS, compensating the repulsive character of nucleonic TBF at high density. The presence of quark matter inside the star is required in order to reach larger maximum masses.

We introduced a density dependent bag parameter $B(\rho)$ in the MIT model in order to explore the maximum NS mass that can be reached in this approach. We compare with calculations using a fixed bag constant and using the color dielectric model. Joining the corresponding EOS with the baryonic one, all three quark models yield maximum masses in the range $(1.5, \ldots, 1.6) M_\odot$, while predicting slightly different radii.

Our results for the maximum masses are in line with other recent calculations of neutron star properties employing various phenomenological relativistic mean field nuclear EOS

together with either effective mass bag model [61] or Nambu-Jona-Lasinio model [54,55] EOS for quark matter.

The value of the maximum mass of neutron stars obtained according to our analysis appears rather robust with respect to the uncertainties of the nuclear and the quark matter EOS. Therefore, the experimental observation of a very heavy ($M \gtrsim 1.7 M_{\odot}$) neutron star, as claimed recently by some groups [62] ($M \approx 2.2 M_{\odot}$), if confirmed, would suggest that either serious problems are present for the current theoretical modeling of the high-density phase of nuclear matter, or that the assumptions about the phase transition between hadron and quark phase are substantially wrong. In both cases, one can expect a well defined hint on the high density nuclear matter EOS.

[1] P. Haensel, *Final Stages of Stellar Evolution*, edited by J.-M. Hamenry and C. Motch, EAS Publication Series (EDP Sciences, 2003); J.M. Lattimer and M. Prakash, Astrophys. J. **550**, 426 (2001).

[2] N. K. Glendenning, *Compact Stars, Nuclear Physics, Particle Physics, and General Relativity*, 2nd ed., 2000 (Springer, New York, 2000).

[3] M. Baldo, I. Bombaci, and G.F. Burgio, Astron. Astrophys. **328**, 274 (1997); X.R. Zhou, G.F. Burgio, U. Lombardo, H.-J. Schulze, and W. Zuo, Phys. Rev. C **69**, 018801 (2004).

[4] A. Akmal, V.R. Pandharipande, and D.G. Ravenhall, Phys. Rev. C **58**, 1804 (1998).

[5] R.A. Hulse and J.H. Taylor, Astrophys. J. Lett. **195**, L51 (1975).

[6] M. Baldo, *Nuclear Methods and the Nuclear Equation of State* (World Scientific, Singapore, 1999).

[7] H.Q. Song, M. Baldo, G. Giansiracusa, and U. Lombardo, Phys. Rev. Lett. **81**, 1584 (1998); Phys. Lett. B **473**, 1 (2000); M. Baldo and G. F. Burgio, *Microscopic Theory of the Nuclear Equation of State and Neutron Star Structure*, in ''Physics of Neutron Star Interiors,'' edited by D. Blaschke, N. Glendenning, and A. Sedrakian, Lectures Notes in Physics, Vol. 578 (Springer, New York, 2001), pp. 1–30.

[8] R.B. Wiringa, V.G.J. Stoks, and R. Schiavilla, Phys. Rev. C **51**, 38 (1995).

[9] J. Carlson, V.R. Pandharipande, and R.B. Wiringa, Nucl. Phys. **A401**, 59 (1983); R. Schiavilla, V.R. Pandharipande, and R.B. Wiringa, *ibid.* **A449**, 219 (1986).

[10] S. L. Shapiro and S. A. Teukolsky, *Black Holes, White Dwarfs, and Neutron Stars* (Wiley, New York, 1983).

[11] M. Baldo, G.F. Burgio, and H.-J. Schulze, Phys. Rev. C **58**, 3688 (1998); **61**, 055801 (2000).

[12] A. Lejeune, P. Grangé, M. Martzolff, and J. Cugnon, Nucl. Phys. **A453**, 189 (1986); I. Bombaci and U. Lombardo, Phys. Rev. C **44**, 1892 (1991); W. Zuo, I. Bombaci, and U. Lombardo, *ibid.* **60**, 024605 (1999).

[13] P. Maessen, Th. Rijken, and J. de Swart, Phys. Rev. C **40**, 2226 (1989).

[14] H.-J. Schulze, A. Lejeune, J. Cugnon, M. Baldo, and U. Lombardo, Phys. Lett. B **355**, 21 (1995); Phys. Rev. C **57**, 704 (1998).

[15] I. Vidaña, A. Polls, A. Ramos, L. Engvik, and M. Hjorth-Jensen, Phys. Rev. C **62**, 035801 (2000).

[16] P. Danielewicz, R. Lacey, and W.G. Lynch, Science **298**, 1592 (2002).

[17] A. Chodos, R.L. Jaffe, K. Johnson, C.B. Thorn, and V.F. Weisskopf, Phys. Rev. D **9**, 3471 (1974).

[18] H.J. Pirner, G. Chanfray, and O. Nachtmann, Phys. Lett. B **147**, 249 (1984).

[19] E. Witten, Phys. Rev. D **30**, 272 (1984); G. Baym, E.W. Kolb, L. McLerran, T.P. Walker, and R.L. Jaffe, Phys. Lett. B **160**, 181 (1985); N.K. Glendenning, Mod. Phys. Lett. A **A 5**, 2197 (1990).

[20] E. Fahri and R.L. Jaffe, Phys. Rev. D **30**, 2379 (1984).

[21] H. Satz, Phys. Rep. **89**, 349 (1982).

[22] M. Alford and S. Reddy, Phys. Rev. D **67**, 074024 (2003).

[23] G.F. Burgio, M. Baldo, P.K. Sahu, A.B. Santra, and H.-J. Schulze, Phys. Lett. B **526**, 19 (2002); G.F. Burgio, M. Baldo, P.K. Sahu, and H.-J. Schulze, Phys. Rev. C **66**, 025802 (2002).

[24] M.C. Birse, Prog. Part. Nucl. Phys. **25**, 1 (1990).

[25] H.J. Pirner, Prog. Part. Nucl. Phys. **29**, 33 (1992).

[26] M.K. Banerjee, Prog. Part. Nucl. Phys. **31**, 77 (1993).

[27] L.R. Dodd, A.G. Williams, and A.W. Thomas, Phys. Rev. D **35**, 1040 (1987).

[28] J.A. McGovern, Nucl. Phys. **A533**, 553 (1991).

[29] R.G. Leech and M.C. Birse, J. Phys. G **18**, 785 (1992).

[30] T. Neuber, M. Fiolhais, K. Goeke, and J.N. Urbano, Nucl. Phys. **A560**, 909 (1993).

[31] V. Barone, A. Drago, and M. Fiolhais, Phys. Lett. B **338**, 433 (1994).

[32] V. Barone, T. Calarco, and A. Drago, Phys. Lett. B **390**, 287 (1997).

[33] V. Barone and A. Drago, Nucl. Phys. **A552**, 479 (1993).

[34] A. Drago, M. Fiolhais, and U. Tambini, Nucl. Phys. **A609**, 488 (1996).

[35] M. Fiolhais, T. Neuber, and K. Goke, Nucl. Phys. **A570**, 782 (1994).

[36] P. Alberto, M. Fiolhais, B. Golli, and J. Marques, Phys. Lett. B **523**, 273 (2001).

[37] N. Aoki and H. Hyuga, Nucl. Phys. **A505**, 525 (1989).

[38] K. Nishikawa, N. Aoki, and H. Hyuga, Nucl. Phys. **A534**, 573 (1991).

[39] M.S. Bae and J.A. McGovern, J. Phys. G **22**, 199 (1996).

[40] J.A. McGovern, M.C. Birse, and D. Spanos, J. Phys. G **16**, 1561 (1990).

[41] W. Broniowski, M. Cibej, M. Kutschera, and M. Rosina, Phys. Rev. D **41**, 285 (1990).

[42] S.K. Ghosh and S.C. Phatak, J. Phys. G **18**, 755 (1992); Phys. Rev. C **52**, 2195 (1995).

[43] V. Barone and A. Drago, J. Phys. G **21**, 1317 (1995).

[44] A. Drago, M. Fiolhais, and U. Tambini, Nucl. Phys. **A588**, 801 (1995).

[45] W.M. Alberico, A. Drago, and C. Ratti, Nucl. Phys. **A706**, 143 (2002).

[46] S.K. Ghosh, S.C. Phatak, and P.K. Sahu, Z. Phys. A **352**, 457 (1995).

[47] A. Drago, U. Tambini, and M. Hjorth-Jensen, Phys. Lett. B **380**, 13 (1996).
[48] A. Drago and A. Lavagno, Phys. Lett. B **511**, 229 (2001).
[49] A. Drago and U. Tambini, J. Phys. G **25**, 971 (1999).
[50] M. Malheiro, E.O. Azevedo, L.G. Nuss, M. Fiolhais, and A.R. Taurines, hep-ph/0111148.
[51] M. Malheiro, M. Fiolhais, and A.R. Taurines, J. Phys. G **29**, 1045 (2003).
[52] U. Heinz and M. Jacobs, nucl-th/0002042; U. Heinz, Nucl. Phys. **A685**, 414 (2001).
[53] Z. Fodor and S.D. Katz, hep-lat/0402006.
[54] M. Buballa, hep-ph/0402234; M. Buballa, F. Neumann, M. Oertel, and I. Shovkovy, nucl-th/0312078.
[55] K. Schertler, S. Leupold, and J. Schaffner-Bielich, Phys. Rev. C **60**, 025801 (1999).
[56] N.K. Glendenning, Phys. Rev. D **46**, 1274 (1992).
[57] M. Alford, K. Rajagopal, S. Reddy, and F. Wilczek, Phys. Rev. D **64**, 074017 (2001).
[58] J.W. Negele and D. Vautherin, Nucl. Phys. **A207**, 298 (1973).
[59] R. Feynman, F. Metropolis, and E. Teller, Phys. Rev. **75**, 1561 (1949).
[60] G. Baym, C. Pethick, and D. Sutherland, Astrophys. J. **170**, 299 (1971).
[61] K. Schertler, C. Greiner, P.K. Sahu, and M.H. Thoma, Nucl. Phys. **A637**, 451 (1998); K. Schertler, C. Greiner, J. Schaffner-Bielich, and M.H. Thoma, *ibid.* **A677**, 463 (2000).
[62] P. Kaaret, E. Ford, and K. Chen, Astrophys. J. Lett. **480**, L27 (1997); W. Zhang, A.P. Smale, T.E. Strohmayer, and J.H. Swank, *ibid.* **500**, L171 (1998).